Nanoscale

Accepted Manuscript

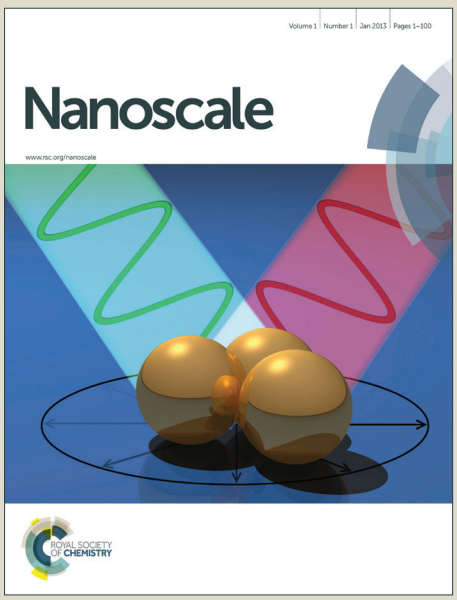

ROYAL SOCIETY OF CHEMISTRY

www.rsc.org/nanoscale

Cite this: DOI: 10.1039/c0xx00000x

www.rsc.org/xxxxxx

COMMUNICATION

Synthesis of TiO_2 Nanosheets via an Exfoliation Route Assisted by Surfactant

Mei Leng,[a] Yu Chen[a] and Junmin Xue*[a]

Received (in XXX, XXX) Xth XXXXXXXXX 20XX, Accepted Xth XXXXXXXXX 20XX

DOI: 10.1039/b000000x

Titanium dioxide (TiO_2) is an important material for photovoltaics, photocatalysis, sensors and lithium ion batteries. Various morphologies of TiO_2 nanomaterials have been synthesized, including zero-dimensional (0D) nanoparticles, one-dimensional (1D) nanowires and nanotubes, as well as three-dimensional (3D) nanostructures. But the two-dimensional (2D) TiO_2 nanostructures, which are expected to have more promising properties and applications, are rarely reported. Herein, we report a surfactant-assisted exfoliation method to synthesize TiO_2 2D nanosheets. It has been revealed that tetrabutylammonium hydroxide (hereafter TBAOH) as a surfactant plays a crucial role in retaining the 2D nanosheet structures. Compared with TiO_2 nanotubes and anatase TiO_2 nanoparticles, the as-prepared TiO_2 single layered nanosheets delivered much higher capacities as an anode of the coin-type Li ion cell, with a reversible capacity of 82.2 mAh g-1 at the 630th cycle at the current density of 2000mA/g.

Recently, two-dimensional (2D) nanosheets composed of one- or a few-layers of atoms, such as graphene and transition metal chalcogenides, have gained great attention owing to their large surface areas and related unique properties[1-10]. The common feature of these 2D nanosheet materials is that their counterpart bulk crystals are layered structures, making it possible to prepare these 2D nanosheets via an exfoliation route. However, it is still a big challenge to synthesize sheet-like structures for those materials with non-layered crystal structures.

Titanium dioxide (TiO_2) is an important material for photovoltaics[11, 12], photocatalysis[11, 13, 14], sensors[14] and lithium ion batteries[15-19]. TiO_2 nanomaterials with various morphologies have been synthesized[11, 16, 20, 21], such as 0D nanoparticles, 1D nanowires and nanotubes, as well as 3D nanostructures. However, the successful fabrication of 2D TiO_2 nanosheets has rarely been reported. Unlike the above mentioned 2D nanomaterials, TiO_2 polymorphs, such as anatase, rutile, brookite, are non-layered crystal structures due to the strong ionic interactions between the metal cations and oxygen anions, therefore, it is hard to prepare TiO_2 2D nanosheets via a conventional exfoliation route. Bottom up chemical synthesis strategy was then proposed to obtain 2D TiO_2 nanosheets. For instance, in 2008, Stucky group reported the successful synthesis of TiO_2 single layer nanosheets through a bottom-up method starting from titanium isopropoxide in a nonaqueous system and with oleylamine as a surfactant [22]. However, it is hard to make the nanosheets in large quantity using such a bottom up synthesis technique. To date, we are still lack of a convenient fabrication method through which TiO_2 nanosheets in large quantity can be synthesized.

Here we report a new exfoliation method to fabricate monolayer TiO_2 nanosheets. The method is inspired from the synthesis method of TiO_2 nanotubes[23-27]. Scheme 1a illustrated the formation process of TiO_2 nanotubes. When TiO_2 crystals are treated with NaOH aqueous solution at an elevated temperature, layered titanates are formed and can be further exfoliated into single layer titanate nanosheets. The resultant nanosheets are instable in morphology due to the existence of dangling bonds such as negatively charged Ti-O- and positively charged Ti- at the sides of the nanosheets. As a result, the titanate nanosheets tend to be rolled up to form nanotubes, which are more stable. In this well established process, titanate nanosheets are actually formed as an intermediate product, which however are hard to be retained due to their instability in morphology. One possible strategy of retaining the titanate nanosheets is to reduce the surface energy of the intermediate nanosheets by introducing a proper surfactant. In this work, the surfactant selected is TBAOH, which is a commonly used cation surfactant and has a large molecule size due to its four butyls. The TBA^+ could attach to the negatively charged Ti-O- bonds on both sides of the nanosheets and thus reduce their surface energy effectively, making the nanosheets stable in the solution.

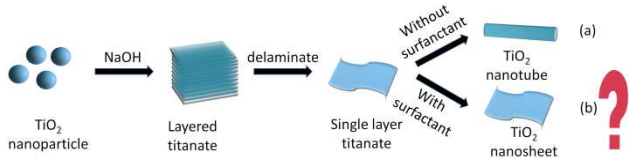

Scheme 1. The strategy of synthesizing TiO_2 nanosheets.

On the basis of the above idea, the synthesis of the targeted TiO_2 nanosheets was conducted in an alkaline solution using anatase TiO_2 nanoparticles (Sigma) as the raw material and TBAOH as the surfactant. The deployed temperature was 130℃ and the reaction time was 24 hours. TiO_2 nanosheets in large quantity (for example, in grams) can be synthesized using this method. Details of the experiments are provided in Supporting Information. The XRD pattern, SEM and TEM images of the raw

TiO_2 nanoparticles were shown in Figure S1. The XRD pattern revealed that the raw TiO_2 nanoparticles were merely anatase with a little rutile (Figure S1a). The particle size of the TiO_2 nanoparticles was about 50 to 200 nm with irregular morphologies, as shown in Figure S1b and S1c. The XRD pattern of the as-prepared TiO_2 nanosheets was shown in Figure S2. It revealed that the crystallinity of the nanosheets was not good. A hump around 25° was observed, corresponding to (101) peak of anatase.

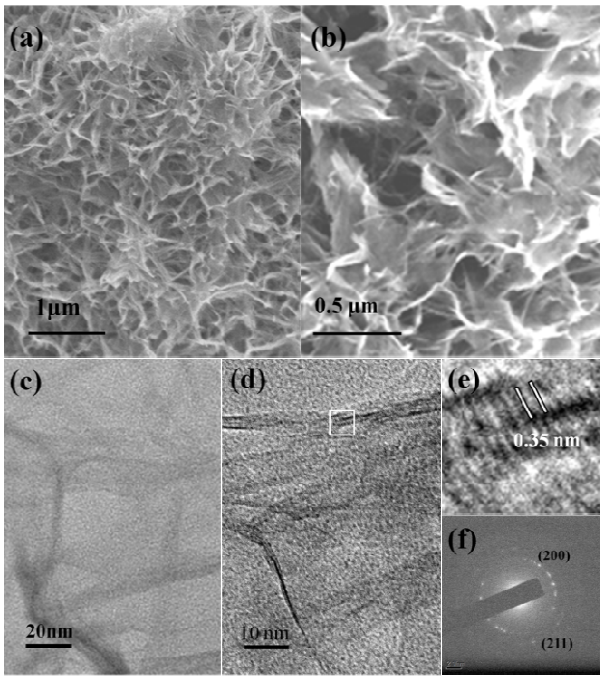

Figure 1. (a) and (b) Low and high magnification SEM images of as-synthesized TiO_2 nanosheets repectively, (c-d) Distinct TEM image of the product, (e) HRTEM of selected by the white frame in (d), (f) the corresponding SAED of the nanosheets in figure (c).

Figure 1 showed distinct SEM and TEM images of the as synthesized TiO_2 nanosheets. From Figure 1a and 1b, it could be seen that the product was the aggregates of nanosheets. To get clear TEM image, the product was dispersed in water with ultrasonic treatment. The TEM image in Figure 1c showed very thin nanosheets with about 200 nm in length and 20 to 50 nm in width. A higher magnification TEM image in Figure 1d revealed that the nanosheets had turn-up edge. The high resolution TEM image of the marked area (white frame) in Figure 1d was shown in Figure 1e. Lattice fringes with a spacing of 0.35 nm, corresponding to the $d_{(101)}$ of the anatase phase, were clearly observed from the turn-up edge of the nanosheets, which indicated that the nanosheets grew along [101] direction. The sample was further characterized using SAED and Raman. Figure 1f was an electron diffraction pattern obtained by focusing the electron beam on the sample of Figure 1c. The pattern was composed of imperfect rings with discrete points, which could be indexed as anatase (200) and (211) planes, respectively. Raman spectrum of the as-prepared nanosheets was shown in Figure S3. The main peaks, 200 cm^{-1}, 394 cm^{-1}, 515 cm^{-1}, 637 cm^{-1} were the typical Raman bands of anatase, confirming the formation of anatase. The thickness of the obtained TiO_2 nanosheets was further characterized using TEM. As shown in the Inset in Figure 2a, the thickness of TiO_2 nanosheet was about 0.40 nm, which was very close to the height of one layer of [TiO_6] octahedron (0.38 nm, Figure 2b). This result suggested that the obtained TiO_2 nanosheets were single layered. AFM was also used to characterize the thickness of TiO_2 nanosheet. However, the as-obtained TiO_2 nanosheets were hard to be fully dispersed during the AFM testing. As shown in Figure S4, a thickness of 0.952 nm was obtained. Such value is larger than the theoretical thickness of a two-layer TiO_2 nanosheet, indicating the loose restacking of two individual TiO_2 nanosheets.

In order to understand the formation process and mechanism of TiO_2 nanosheets, the effects of the experiment parameters on the formation of TiO_2 nanosheets were further investigated. It was no doubt that TBAOH played a key role in the synthesis of the TiO_2 nanosheets. As can be seen from Figure S5, the resulting products showed a strong dependence on the amount of TBAOH at 130 °C . When there was no TBAOH, the products were the mixture of nanotubes and unreacted nanoparticles (Figure S5a). When 4 g of TBAOH was added, there were nanosheets formed in the product, as well as nanotubes and unreacted nanoparticles (Figure S5b). Further increasing the amount of TBAOH to 8 g, as shown in Figure S5c, nanotubes were nearly disappeared and only nanosheets and unreacted nanoparticles existed in the product. According to the formation mechanism of TiO_2 nanotubes reported by the previous papers, the single layer nanosheet will roll up to nanotube if there was no TBAOH. Obviously, TBAOH, as a surfactant, effectively prevent the formation of nanotubes and thus promote the formation of nanosheets.

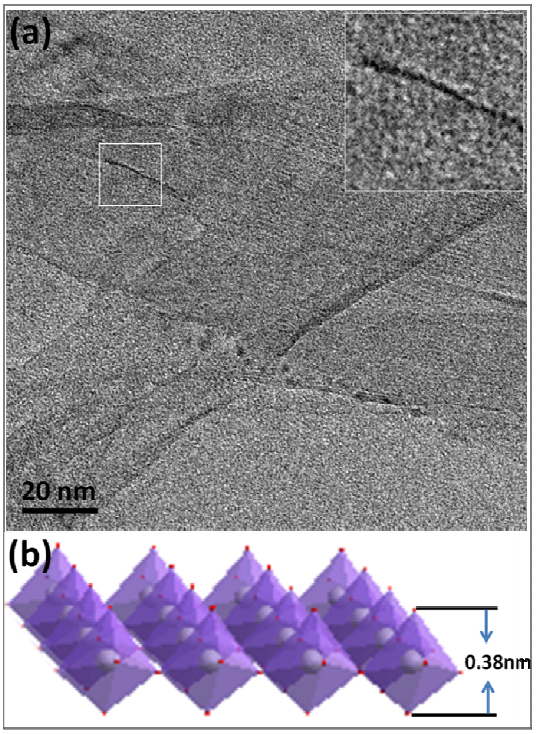

Figure 2. (a) TEM image of TiO_2 nanosheet and a magnified image of white rectangle region in (a)(Inset), (b) a model of a layer [TiO_6] octahedron(red ball stands for oxygen atom and white ball stands for titanium atom).

Samples synthesized at different durations and temperatures

were collected when the amount of TBAOH was fixed at 8 g. For the sample treated at 130 °C for 4 h (Figure 3b), layered structures were formed on the surfaces of nanoparticles, as compared to the smooth surface of the raw nanoparticles (Figure

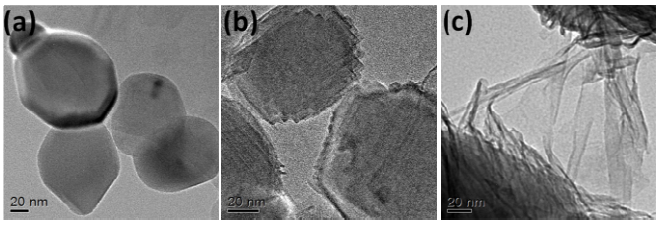

Figure 3. TEM images of samples collected at different times (a) 0 min, (b) 4 h, (c) 12 h.

3a). This indicated that layered titanates were formed upon the reaction between NaOH and TiO_2. Some single-layer nanosheets were even observed surrounding the nanoparticles, suggesting that the formed layered titanates tended to be delaminated from the mother particles. As the reaction time was prolonged to 12h, more nanosheets were formed, which were closely bound up with the TiO_2 nanoparticles (Figure 3c). With increasing the reaction time to 24 hours, most of the TiO_2 nanoparticles disappeared and TiO_2 nanosheets were formed almost completely (as shown in Figure 1). Temperature dependent experiments were carried out by varying the reaction temperature from 80 °C, 130 °C to 180 °C. The reaction time was fixed at 24 hours and the amount of surfactant is 8 g. When the reaction was carried out at 80 °C, a few nanosheets were formed, as shown in Figure S6a. However, if the reaction temperature was too high, such as 180 °C, the product only consisted of nanobelts instead of nanosheets (Figure S6b). At such a high temperature, single layer nanosheets tend to be stacked together to become more stable even in the presence of surfactant. From these studies, it was concluded that the moderate temperature (130 °C) was critical to synthesize the single-layer nanosheets.

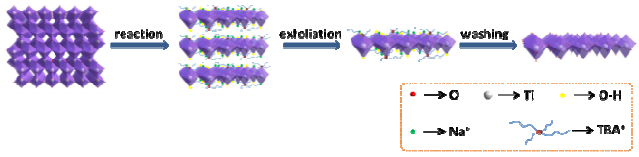

Scheme 2. The formation mechanism of TiO_2 nanosheets.

According to the discussion above, our idea of synthesizing TiO_2 nanosheets by introducing a surfactant to retain the intermediate titanate nanosheets was proved to be feasible. The more detailed formation mechanism was illustrated in Scheme 2. The crystalline structure (anatase) of TiO_2 is on the basis of TiO_6 octahedra, which share vertices and edges to build up the three-dimensional framework. During the alkali-hydrothermal process, the Ti–O–Ti bonds were broken and the intermediate titanate layered structures with positively charged Ti– dangling bonds and negatively charged Ti–O– dangling bonds were formed. The XRD pattern in Figure S2 verified the formation of titanate. Upon the addition of TBAOH surfactant, TBA^+ ions, together with OH^- and Na^+ ions, bond with these dangling bonds to neutralize the charge. Therefore, the surface energy of the intermediate titanate nanosheets was reduced and thus the rolling up process was stopped. With the reaction proceeded, more and more Ti–O–Ti bonds were broken and the resulting nanosheets started to peel off from the nanoparticles. Upon washing with acids such as HCl or HNO_3, the cations on the nanosheets were removed, and thus the titanate nanosheets were changed into TiO_2 nanosheets. To demonstrate the promising properties of 2D TiO_2 nanosheets, the as-obtained TiO_2 nanosheets were fused as the anode material and assembled into a CR2106 coin-type cell for electrochemical

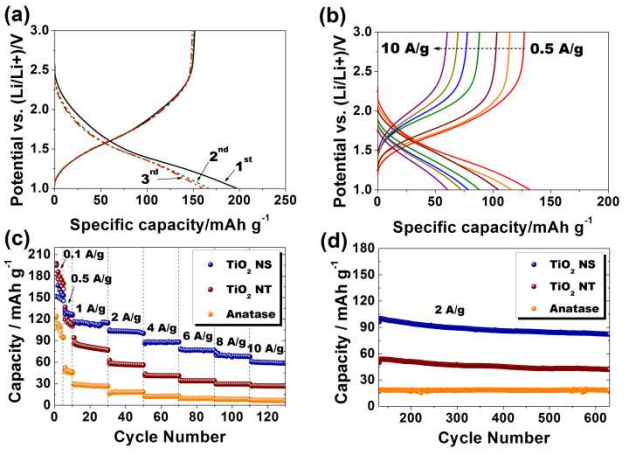

Figure 4. Electrochemical performances of TiO_2 nanosheets (NS), TiO_2 nanotubes (NT), and anatase particles (raw material). Charge/discharge profiles of TiO_2 NS at (a) current densities of 100 mA g^{-1} and (b) higher rates from 500 to 10000 mA g^{-1}. (c) Rate capability tests from 100 to 10000 mA g^{-1} and (d) subsequent cycling tests at 2000 mA g^{-1} of TiO_2 NS (blue), TiO_2 NT (red), and anatase particles (orange).

tests. The charge/discharge profiles of TiO_2 nanosheets under the current density of 100 mA g^{-1} at the first three cycles were shown in Figure 4a. The first discharge and charge capacities were 197.6 and 151.6 mAh g^{-1}, respectively, demonstrating an initial coulombic efficiency of 79.3%. Such value is comparable to those reported efficiencies in literature for TiO_2 in anode applications[19]. In the subsequent two cycles, the coulombic efficiency of TiO_2 nanosheets quickly rose to above 90%, with stable reversible capacities of 150.8 and 149.1 mAh g^{-1}, respectively. No evident potential plateau was observed in these charge/discharge profiles, which has also been demonstrated in the electrochemical studies of other two-dimensional materials, such as graphene[8] and MoS_2[28]. The TiO_2 nanosheets anode was further tested with increasing current densities up to 10000 mA g^{-1}. The corresponding charge/discharge profiles were shown in Figure 4b. As comparison, anodes fabricated from TiO_2 nanotubes and anatase nanoparticles (raw material) were also tested under the same condition. Despite the fact that TiO_2 nanotubes demonstrated a slightly higher first cycle capacity of 183.5 mAh g^{-1}, TiO_2 nanosheets showed much superior electrochemical performances at high current densities. For instance, as shown in Figure 4c, the reversible capacity of TiO_2 nanotubes was quickly faded to 80.4 mAh g^{-1} at the current density of 1000 mA g^{-1}. In contrast, TiO_2 nanosheets delivered a reversible capacity of 111.7 mAh g^{-1} at the same current density. The reversible capacities of TiO_2 nanosheets were 127.2, 114.4, 103.3, 85.8, 77.7, 69.8, and 60.4 mAh g^{-1} at the current densities of 500, 1000, 2000, 4000, 6000, 8000, and 10000mA g^{-1}, respectively, showing minor drops in capacities as current density increased. The TiO_2 particles showed much inferior

electrochemical performances as compared to the nanotubes and nanosheets, delivering only 6.9 mAh g^{-1} at the current density of 10000 mAh g^{-1}. The cells were subjected to further cycling test at a current density of 2000 mA g^{-1} for 630 cycles. As shown in Figure 4d, stable reversible capacities were achieved by all three materials. Among them, TiO_2 nanosheets delivered much higher capacities than the other two, with a reversible capacity of 82.2 mAh g^{-1} at the 630th cycle.

In conclusion, a new exfoliation method for producing single layer TiO_2 nanosheets was reported, which was developed from a well established TiO_2 nanotube synthesis process. By adding a surfactant TBAOH, the intermediate titanate nanosheets were retained and thus the formation of TiO_2 nanosheets was promoted. The obtained TiO_2 nanosheets showed promising applications as Li ion battery anode, demonstrating better electrochemical performance than TiO_2 nanotubes and anatase nanoparticles. TiO_2 nanosheets in large quantity can be fabricated through this exfoliation method.

This work is financially supported by MOE's Singapore FRC Grant WBS R-284-000-102-112 and R-265-000-124-112.

Notes and references

[a] *A Department of Materials Science and Engineering, National University of Singapore, Singapore. Fax: +65 6776 3604; Tel: +65 6516 4655; E-mail: msexuejm@nus.edu.sg*

† Electronic Supplementary Information (ESI) available: [Detailed experimental procedures, results of XRD, SEM, Raman and TEM.]. See DOI: 10.1039/b000000x/

1. K. S. Novoselov, A. K. Geim, S. V. Morozov, D. Jiang, Y. Zhang, S. V. Dubonos, I. V. Grigorieva and A. A. Firsov, Science, 2004, 306, 666-669.
2. M. Xu, T. Liang, M. Shi and H. Chen, Chemical Reviews, 2013, 113, 3766-3798.
3. C. N. R. Rao, H. S. S. Ramakrishna Matte and U. Maitra, Angewandte Chemie International Edition, 2013, 13162-13185.
4. M. Naguib, J. Halim, J. Lu, K. M. Cook, L. Hultman, Y. Gogotsi and M. W. Barsoum, Journal of the American Chemical Society, 2013, 135, 15966-15969.
5. M. R. Lukatskaya, O. Mashtalir, C. E. Ren, Y. Dall'Agnese, P. Rozier, P. L. Taberna, M. Naguib, P. Simon, M. W. Barsoum and Y. Gogotsi, Science, 2013, 341, 1502-1505.
6. X. Li, X. Hao, M. Zhao, Y. Wu, J. Yang, Y. Tian and G. Qian, Advanced Materials, 2013, 25, 2200-2204.
7. J. H. Han, S. Lee and J. Cheon, Chemical Society Reviews, 2013, 42, 2581-2591.
8. R. Mukherjee, A. V. Thomas, A. Krishnamurthy and N. Koratkar, ACS Nano, 2012, 6, 7867-7878.
9. Y. Zhu, S. Murali, W. Cai, X. Li, J. W. Suk, J. R. Potts and R. S. Ruoff, Advanced Materials, 2010, 22, 3906-3924.
10. R. Ma and T. Sasaki, Advanced Materials, 2010, 22, 5082-5104.
11. T. Froschl, U. Hormann, P. Kubiak, G. Kucerova, M. Pfanzelt, C. K. Weiss, R. J. Behm, N. Husing, U. Kaiser, K. Landfester and M. Wohlfahrt-Mehrens, Chemical Society Reviews, 2012, 41, 5313-5360.
12. W. Yang, J. Li, Y. Wang, F. Zhu, W. Shi, F. Wan and D. Xu, Chemical Communications, 2011, 47, 1809-1811.
13. Y. H. Hu, Angewandte Chemie International Edition, 2012, 51, 12410-12412.
14. W. Zhou, G. Du, P. Hu, G. Li, D. Wang, H. Liu, J. Wang, R. I. Boughton, D. Liu and H. Jiang, Journal of Materials Chemistry, 2011, 21, 7937.
15. S.-T. Myung, M. Kikuchi, C. S. Yoon, H. Yashiro, S.-J. Kim, Y.-K. Sun and B. Scrosati, Energy & Environmental Science, 2013, 6, 2609-2614.
16. C. Jiang and J. Zhang, Journal of Materials Science & Technology, 2013, 29, 97-122.
17. H. B. Wu, X. W. Lou and H. H. Hng, Chem.-Eur. J., 2012, 18, 3132-3135.
18. S. Liu, H. Jia, L. Han, J. Wang, P. Gao, D. Xu, J. Yang and S. Che, Advanced Materials, 2012, 24, 3201-3204.
19. V. Gentili, S. Brutti, L. J. Hardwick, A. R. Armstrong, S. Panero and P. G. Bruce, Chemistry of Materials, 2012, 24, 4468-4476.
20. X. Chen and S. S. Mao, Chemical Reviews, 2007, 107, 2891-2959.
21. D. V. Bavykin, J. M. Friedrich and F. C. Walsh, Advanced Materials, 2006, 18, 2807-2824.
22. B. Wu, C. Guo, N. Zheng, Z. Xie and G. D. Stucky, Journal of the American Chemical Society, 2008, 130, 17563-17567.
23. B. D. Yao, Y. F. Chan, X. Y. Zhang, W. F. Zhang, Z. Y. Yang and N. Wang, Applied Physics Letters, 2003, 82, 281-283.
24. C.-C. Tsai and H. Teng, Chemistry of Materials, 2005, 18, 367-373.
25. Q. Chen, W. Zhou, G. H. Du and L. M. Peng, Advanced Materials, 2002, 14, 1208-1211.
26. G. H. Du, Q. Chen, R. C. Che, Z. Y. Yuan and L. M. Peng, Applied Physics Letters, 2001, 79, 3702-3704.
27. T. Kasuga, M. Hiramatsu, A. Hoson, T. Sekino and K. Niihara, Advanced Materials, 1999, 11, 1307-1311.
28. J.-Z. Wang, L. Lu, M. Lotya, J. N. Coleman, S.-L. Chou, H.-K. Liu, A. I. Minett and J. Chen, Adv. Energy Mater., 2013, 3, 798-805.